Received: 19 October 2020 | Accepted: 17 March 2021

DOI: 10.1111/gcbb.12838

GCB-BIOENERGY BIOPRODUCTS FOR A SUSTAINABLE BIOECONOMY Open Access

WILEY

ORIGINAL RESEARCH

Adapting the CROPGRO model to simulate growth and production of *Brassica carinata*, a bio-fuel crop

Kenneth J. Boote[1] | **Ramdeo Seepaul**[2] | **Michael J. Mulvaney**[3] | **Austin K. Hagan**[4] | **Mahesh Bashyal**[3] | **Sheeja George**[2] | **Ian Small**[2] | **David L. Wright**[2]

[1]Department of Agricultural and Biological Engineering, University of Florida, Gainesville, FL, USA

[2]North Florida Research and Education Center, University of Florida, Quincy, FL, USA

[3]West Florida Research and Education Center, University of Florida, Jay, FL, USA

[4]Auburn University, Auburn, AL, USA

Correspondence
Kenneth J. Boote, Department of Agricultural and Biological Engineering, University of Florida, 1741 Museum Road, Gainesville, FL 32611, USA.
Email: kjboote@ufl.edu

Funding information
National Institute of Food and Agriculture, U.S. Department of Agriculture, Grant/Award Number: 2016-11231

Abstract

Carinata (*Brassica carinata*) is an oilseed crop which, because of its non-edible oil composition and favorable fatty acid profile, is proposed as a "green" sustainable aviation fuel. It can be grown as a winter crop in the southeastern USA or as a summer annual crop in northern latitudes. No crop models exist for carinata because it is a relatively new crop. The CROPGRO model is a mechanistic crop simulation of daily crop growth and development as a function of daily weather, soil properties, crop management, and species parameters. We adapted the CROPGRO model to simulate carinata based on growth analysis data collected over two seasons at three sites: Quincy, FL, Jay, FL, and Shorter, AL. The adaptation process required literature knowledge as well as optimization against field observations. The parameterization of model sensitivities to climatic factors is presented. The adapted model gave good simulations of carinata growth dynamics compared to observed growth during different seasons and locations and in response to N fertilization. While additional testing is appropriate, the model is sufficiently ready to be used for various applications. An example application is presented for the effect of sowing date on carinata yield and maturity over long-term weather in the Southeastern USA.

KEYWORDS

Brassica carinata, crop simulation model, growth analyses, jet fuel, model parameterization, N response

1 | INTRODUCTION

Brassicacarinata (carinata) is a non-food oilseed crop with potential as a "green" biofuel feedstock because its oil properties allow for conversion to jet fuel that is equivalent to petroleum-derived fuels (Cardone et al., 2003). As a non-edible oilseed, carinata is planted in the offseason and does not compete with food crops, while the meal after oil extraction can be processed into a high protein animal feed supplement. The carinata production cycle coincides with wheat (*Triticum aestivum* L.) and other winter-grown crops in the Southeastern USA. Due to low wheat profitability, carinata is an alternative to winter wheat that can be grown on large areas in the Southeast that are typically in winter fallow. So, the opportunity exists for fallow acreage to be cropped with carinata with the goal of providing a local feedstock for processing into sustainable aviation fuel, providing an additional income source for farmers, and serving as a winter-grown crop to recycle nutrients to be released to the following summer crop.

An important aspect of model adaptation is to understand and appreciate the crop being modeled. Carinata is a cool-season crop grown as a summer crop in cool regions or as a winter crop where winter temperatures are not too severe. The native habitat of *B. carinata* is the highland plateaus of Ethiopia, where the crop grows well in cool environments at 14–18°C temperature (Malik, 1990). It is stated by Malik (1990) to be photoperiod-insensitive as well as heat and drought tolerant. Carinata has a low rosette growth habit with minimal early-season stem growth, followed by rapid increases in stem growth and height with the onset of bolting (Seepaul et al., 2021). Its growth habit is determinate, and the main stem and branches end as floral racemes. Despite this determinate growth habit, flowering occurs over a relatively long time period. Pods (siliques) contain 9–12 small seeds per pod. Leaves senesce and abscise relatively early during seed-filling, but the pods are green, capture light, and carry out photosynthesis (Gammelvind et al., 1996). The siliques contribute a considerable amount of assimilates because of their upper canopy position. Carinata as a non-legume is responsive to N fertilization as described by Seepaul et al. (2016), Seepaul, Marois, et al. (2019), Seepaul, Small, et al. (2019).

Crop simulation models have been widely accepted as tools for evaluating crop response to weather, soils, crop management practices, and genetic characteristics (Jones et al., 2017). Mechanistic crop simulation models such as CROPGRO (Boote et al., 1998; Jones et al., 2003) incorporate and synthesize knowledge of crop physiology, phenology, and biology. The CROPGRO model exists within the Decision Support System for Agrotechnology Transfer (DSSAT) software system (Hoogenboom et al., 2019), which provides a convenient system for the input of weather, soils, management, and crop genetic information, as well as handling model output for graphical, statistical, and application purposes. The CROPGRO model has been adapted for 18 species so far, including canola (*B. napus*) which is a winter- or spring-grown food-quality oilseed (Deligios et al., 2013; Jing et al., 2016), closely related to carinata. At present, there are no crop models for carinata; thus, the goal of this research was to adapt the CROPGRO model for carinata.

The CROPGRO model is a mechanistic crop simulation model that simulates daily growth and development as a function of daily weather, soil properties, crop management, and cultivar/species parameters. The model simulates leaf-level photosynthesis and processes related to crop carbon (C) balance, crop-soil nitrogen (N) balance, and crop-soil water balance. Its leaf-level photosynthesis is coupled within a hedgerow light-interception model (Boote & Pickering, 1994) that depends on simulated canopy height, width, and leaf area index (LAI). Leaf-level photosynthesis is parameterized from measured light-saturated leaf rates, and photosynthetic response to CO_2 follows a simplified rubisco kinetics approach from Farquhar and von Caemmerer (1982). The water balance uses the tipping bucket approach of Ritchie (1998), which includes infiltration, runoff, drainage, root water uptake, and soil water evaporation. The evapotranspiration options include the Priestley-Taylor (1972) or FAO-56 methods (Allen et al., 1998). The water balance processes in the DSSAT models are described by Boote et al. (2008). CROPGRO shares the soil N balance modules of DSSAT, and uses either the Godwin (default) or the CENTURY soil organic carbon (SOC) modules. For this paper, we used the CENTURY SOC option (Gijsman et al., 2002), which requires setting the stable fraction of SOC for the respective soils. Jing et al. (2016) reported that the CENTURY option gave better performance under zero N fertilization for the CROPGRO-Canola model. The plant N balance processes in CROPGRO are described by Boote et al. (2009).

CROPGRO (Boote et al., 1998) is a generic model with one common FORTRAN code for multiple species that uses input files to define species traits and cultivar characteristics, thus allowing easy adaptation to simulate the growth dynamics for a number of crops, including the legumes and non-legumes. CROPGRO model adaptations include fababean (*Vicia faba* L.) (Boote et al., 2002) and pigeonpea (*Cajanus cajan* (L.) Millsp.; Alderman et al., 2015), as well as non-legumes such as tomato (*Solanum lycopersicum* L.; Boote et al., 2012), safflower (*Carthamus tinctorium* L.; Singh et al., 2015), and canola (*Brassica napus* L.; Deligios et al., 2013; Jing et al., 2016). The adaptation process requires the relationships and parameters in the species, ecotype, and cultivar files to be based on literature knowledge and parameterized based on measured growth and yield data collected from field experiments. A further advantage of starting with an existing model is that all the ancillary input/output files for entry of weather, soils, management, and genetic information are already present, along with the graphical and statistical analysis of output files.

At present, there are no crop models for carinata, but having a model adapted for carinata would provide a tool for evaluating crop response to weather, soils, management, and genetic improvement. Therefore, the objective of this research was to adapt the CROPGRO model for carinata based on growth analysis data collected over two seasons at three sites in the Southeastern US. We started with the parameters of the existing CROPGRO-Canola model in DSSAT, because canola is a similar cool-season species with relatively low cardinal temperatures for the processes of phenology, photosynthesis, pod addition, and seed growth.

2 | MATERIALS AND METHODS

2.1 | Field experiments for growth analysis data collection

Field experiments were conducted at three sites (Quincy, FL; Jay, FL; and Shorter, AL) over two seasons (2017–2018; and 2018–2019), during which in-season growth was measured

(Table 1). There were four replications, and individual plot sizes were 1.50 × 7.62 m at Quincy, 1.43 × 7.62 m at Shorter, and 7.32 × 10.67 m at Jay. At the Quincy and Shorter sites, two cultivars (Avanza 641 and AX17012) were sampled, while at Jay, FL, only Avanza 641 was sampled. Table 1 lists the latitude, longitude, soil type, sowing dates for each year, plant density (measured at harvest), and N fertilization. Detailed in-season data at the Jay site were collected on the 90 kg N ha^{-1} rate treatment, which was part of a larger experiment on N fertilization rates (0, 45, 90, 135, and 180 kg N ha^{-1}) from which total biomass, total N mass, and vegetative N concentration data from all five treatments were used to evaluate simulated N response variables. The sowing dates, soil, and plant density of the larger Jay N rate experiment are in Table 1. The water-holding characteristics, soil organic carbon, and initial conditions for the three soils are provided in Table 2. Weather data were taken from weather stations on-site at Quincy and Jay, while weather for the Shorter, AL site was accessed from NASA's POWER database. Sites were rainfed except for one irrigation of 15.2 mm applied on March 20, 2019 at Quincy, and one irrigation of 19.0 mm applied on November 13, 2017 for establishment at Jay.

Growth analysis sampling varied by location. At all locations, total biomass samples were collected at 2–3 week intervals, from three of 1 m length of row at Quincy where row spacing was 0.305 m (0.9144 m^2 sampled), two of 1 m length of row at Jay and Shorter where the row spacing was 0.381 m at Jay (0.762 m^2 sampled), and 0.356 m at Shorter (0.7112 m^2). Quincy was an exception to this principle for mid-season samples in year 1, when only 10 plants were sampled on February 28 and then five plants on March 14 and 28, 2018 (due to workload). This unfortunately caused upward bias in weight per plant for those dates. Multiplying weight per plant by plant population was a poor option because up to half of the plants died over the course of the season (typical of all sites and seasons, and this was *not* caused by "winterkill"). The plants sampled were not representative of the average plant, possibly because the human tendency is to ignore smaller "less typical" plants during sampling. Therefore, we bias-corrected those three dates in 2017–2018 at Quincy by using the 0.9144 m^2 samples from the last four dates and their recorded plant population. The bias correction factor was average weight per plant (from last four 0.9144 m^2 samples) divided by the weight per plant of the 5 or 10 plant samples collected on February 28, March 14, and March 28, 2018. The bias correction averaged over those three dates was 0.662 for Avanza-641, and 0.730 for AX17012. No bias corrections were necessary for Jay, Shorter, or the 2018–2019 season at Quincy. For Quincy and Jay, subsampled plants were separated into leaf, stem, and pod, which allowed computing leaf, stem, and pod fractions. At Quincy, pods were separated into seeds and podwall, to compute fraction seed (HI), and shelling percent (seed*100/(seed + pod)). Leaf area was measured with an LI-3100 leaf area meter, and specific leaf area (SLA) was computed as leaf area (cm^2) divided by leaf mass (g). The leaf, stem, pod, and seed mass as kg ha^{-1} and LAI were computed from the fractions and SLA of the subsamples multiplied by the total biomass (kg ha^{-1}) of the large sample. Nondestructive LAI was measured with the LA-2200 canopy analyzer (LI-COR Biosciences) at Jay in 2018–2019 season. At Jay, 0.762 m^2 samples for biomass were taken from all five N rate treatments, but the fraction and ratio data were collected only from subsamples from the 90 kg N ha^{-1} treatment. Computed leaf, stem, and pod mass were calculated for all five N rate treatments based on the assumption that the fractions and ratios were the same for all N rate treatments. For the Jay site, vegetative N concentration and total N accumulation were measured for all N rate treatments.

2.2 | Adapting the CROPGRO model: Methods and statistics

The necessary files were created for running the DSSAT software. The management information (sowing date, row spacing, plant population, fertilization, irrigation, prior crop residue, initial nitrate and ammonium concentrations, soil type, cultivar, and CENTURY soil organic C method) were entered into the File X (management file). The collected growth data were entered into end-of-season and time-series files.

TABLE 1 Location, soil type, sowing date, plant density at harvest, and N application during two seasons at three sites

Site	Latitude/Longitude	Soil type	Sowing date	Plant density (plants m^{-2})	N applied (kg N ha^{-1})
Quincy, FL	30.60N, 84.40W	Norfolk sandy loam	4 December 2017	63.0	89 (2 splits)
Quincy, FL	30.60N, 84.40W	Norfolk sandy loam	9 January 2019	50.0	111 (2 splits)
Jay, FL	30.78N, 87.14W	Red Bay sandy loam	2 November 2017	37.1	90 (2 splits)
Jay, FL	30.78N, 87.14W	Red Bay sandy loam	12 December 2018	16.0	90 (2 splits)
Shorter, AL	32.44N, 85.90W	Eustis loamy sand	16 November 2017	93.3	124 (3 splits)
Shorter, AL	32.44N, 85.90W	Eustis loamy sand	1 February 2019	36.0	90 (3 splits)

TABLE 2 Soil profile properties and initial conditions of inorganic N for Quincy, FL., Jay, FL., and Shorter, AL. Initial inorganic N are reported values for Quincy and Jay, but are outcomes of CENTURY spin-up for Shorter, AL

Depth	SLOC	Initial N		SLLL	SDUL	SSAT	SRGF	SSKS
cm	%	g Mg^{-1}		cm^3 [water]/cm^3[soil]				cm h^{-1}
		NH_4	NO_3					
Norfolk Sandy Loam (Quincy, FL)								
5	1.16	0.2	10.6	0.101	0.249	0.498	1.000	1.32
15	1.16	0.2	4.3	0.101	0.249	0.498	1.000	1.32
25	1.16	0.2	3.3	0.101	0.249	0.498	1.000	1.32
43	0.30	0.1	1.4	0.173	0.303	0.439	0.400	0.23
66	0.30	0.0	0.6	0.173	0.303	0.439	0.400	0.23
91	0.13	0.0	0.6	0.203	0.329	0.444	0.210	0.23
127	0.07	0.0	0.4	0.212	0.333	0.437	0.110	0.23
142	0.13	0.0	0.4	0.214	0.339	0.444	0.070	0.23
203	0.07	0.0	0.4	0.205	0.316	0.422	0.040	0.23
Red Bay sandy loam (Jay, FL)								
15	0.89	1.3/1.4[a]	4.1/2.2[a]	0.103	0.218	0.326	1.000	2.59
20	0.89	0.8/1.0	2.1/1.5	0.103	0.218	0.326	1.000	2.59
35	0.32	0.8/1.0	2.1/1.5	0.125	0.239	0.333	0.600	2.59
60	0.04	0.8/1.0	2.1/1.5	0.147	0.261	0.337	0.100	0.43
90	0.04	0.8/1.0	2.1/1.5	0.147	0.261	0.337	0.100	0.43
128	0.04	0.8/1.0	2.1/1.5	0.147	0.261	0.337	0.100	0.43
150	0.02	0.8/1.0	2.1/1.5	0.125	0.236	0.332	0.020	2.59
Eustis loamy sand (Shorter, AL)								
5	0.94	0.3	0.8	0.055	0.177	0.302	1.00	33
15	0.94	0.1	1.3	0.055	0.177	0.302	1.00	33
18	0.94	0.1	3.1	0.055	0.177	0.302	1.00	33
30	0.5	0.1	2.5	0.055	0.177	0.302	0.85	33
45	0.5	0.1	3.8	0.055	0.177	0.302	0.85	33
60	0.3	0.1	4.5	0.055	0.177	0.302	0.40	33
90	0.3	0.0	4.6	0.054	0.172	0.313	0.30	33
120	0.2	0.0	3.6	0.054	0.172	0.313	0.20	33
147	0.2	0.0	2.6	0.054	0.172	0.313	0.20	33
172	0.1	0.0	3.0	0.054	0.172	0.313	0.15	33

Abbreviations: NH_4, ammonium; NO_3, Nitrate; SDUL, soil water content at drained upper limit; SLLL, soil water content at lower limit of plant extractable soil water; SLOC, soil organic carbon; SRGF, soil root growth factor, 0.0 to 1.0; SSAT, Soil water content at saturation; SSKS, Sat. hydraulic conductivity.

[a]Values in year 1 and year 2 for Jay.

The model adaptation followed a logical sequence as described by Boote et al. (2002) for adaptation of CROPGRO for faba bean (*Vicia faba*). The following approach was used: (1) values and relationships from the literature were used where available, (2) simulated outputs were compared to observed time-series data from the carinata experiments and model parameters optimized to improve the statistical fit. The adaptation involved setting tissue compositions, and especially the shape of temperature-dependent processes for the rate of leaf appearance, rate of progress to phenological events, photosynthesis, pod addition, and seed growth rate, all parameterized in the species file of CROPGRO. Cultivar parameters adjusted include photothermal phase durations, duration to end of leaf area expansion, duration of pod addition, leaf photosynthesis, seed size, seed protein, seed lipid, and single seed-filling duration. The GBUILD graphical interface of DSSAT computes observed and simulated means, root mean square error (RMSE), and *d*-statistic of model fit. These were used, along with visual evaluation, to guide the model adaptation process. Because carinata is related to canola (also a winter-grown cool-season oilseed crop), we used an existing template from the CROPGRO-Canola model (V4.6.5, Hoogenboom et al., 2015) as the starting point followed by modification of the species, ecotype, and cultivar files. There were multiple iterations in a

general sequence: (1) entering composition and literature values; (2) simulating phenology timing (cultivar parameters); (3) simulating biomass accumulation, LAI, and specific leaf area (based on species and cultivar parameters); (4) simulating biomass partitioning among leaf, stem, and root tissue (mostly based on species parameters) and iteration to adjust LAI and biomass; (5) simulating the onset, partitioning intensity, and duration of the pod and seed growth (using cultivar parameters); (6) setting leaf and stem protein thresholds and N mobilization (species parameters) to mimic vegetative N concentration over time. There was considerable iteration among the listed parameters associated with: (1) modification of cardinal temperatures for photosynthesis, leaf appearance rate, pod addition, and seed growth to mimic growth during cold winter periods or warm late spring; and (2) adjusting the stable soil organic carbon pool (SOM3) for all three sites, especially for the N response treatments at Jay. The SOM3 pool was calibrated to be 0.76, 0.78, and 0.83 as a fraction of the total SOC at Quincy, Jay, and Shorter, respectively.

Carinata model adaptation proceeded along the prior described sequence, via manually modifying parameters (no automated algorithm was used). Model performance during successive steps was evaluated based on visual plotting of time-series outputs against observations, giving equal consideration to both root mean square error (RMSE; Equation 1) and the Willmott agreement index (*d*-statistic; Equation 2; Willmott, 1982; Willmott et al., 1985).

$$\mathrm{RMSE} = \sqrt{\frac{1}{N}\sum_{i=1}^{N}\left(Y_i - \widehat{Y}_i\right)^2} \quad (1)$$

where N is the total number of data points for comparison, Y_i are the observed values, and $\widehat{Y}_i$ are the simulated values. A smaller RMSE represents a better model prediction. The Willmott agreement index is given by:

$$d = 1 - \left[\frac{\sum_{i=1}^{N}\left(Y_i - \widehat{Y}_i\right)^2}{\sum_{i-1}^{N}\left(\left|\widehat{Y}_i - \dot{Y}\right| + \left|Y_i - \dot{Y}\right|\right)^2}\right], 0 \le d \le 1 \quad (2)$$

where N is the total number of data points for comparison, Y_i are the observed values, $\widehat{Y}_i$ are the simulated values, and $\dot{Y}$ is the mean of the observed data. For good model prediction, the d index should be near 0.90, that is, close to 1.

2.3 | A regional application of the CROPGRO-Carinata model

One of the reasons for developing the CROPGRO-Carinata model is to evaluate management strategies such as sowing date that affect yield response in the Southeastern USA. Long-term weather data (1984–2019) were accessed for eight sites: Quincy and Jay (Florida), Tifton, Midville, and Plains (Georgia), and Shorter, Brewton, and Fairhope (Alabama). The respective soils for these sites were: Norfolk sandy loam (Quincy), Red Bay sandy loam (Jay), Tifton loamy sand (Tifton), Clarendon sandy loam (Midville), Faceville sandy clay loam (Plains), Eustis loamy sand (Shorter), Benndale fine sandy loam (Brewton), and Marlboro very fine sandy loam (Fairhope). Available volumetric water-holding capacity was in the range of 10%–13%, except for the Marlboro soil which had 14%–15% available water. The CENTURY organic carbon module was used, and the fraction SOM3 ranged from 0.78 to 0.85, mostly at 0.80. Model simulations were initiated with the profile at field capacity, and the initial soil inorganic nitrate and ammonium, and amount of residue incorporated prior to sowing were assumed the same as that used at Jay, FL. Following recommendations for economic optimum N rate (Seepaul, Marois, et al., 2019), N fertilization of 33 kg N ha^{-1} was applied at sowing and 57 N kg ha^{-1} at 78 days after sowing. Plant population of 48 plants m^{-2} was used (average of six trials in Table 1). Sowing dates of October 16, November 6, November 27, December 18, January 9, and January 30 were simulated to determine effect on seed yield and maturity dates over long-term weather (35 seasons).

3 | RESULTS AND DISCUSSION

3.1 | Model adaptation — Cardinal temperature relationships

Starting with the CROPGRO-Canola model, changes were made in functions that described temperature dependency of simulated processes. Table 3 contrasts the temperature dependencies of the CROPGRO-Carinata model to those used for CROPGRO-Canola. This comparison is valuable because canola is a similar species for which there is more published data, and also because the CROPGRO-Canola model has been evaluated for several environments. The rate of leaf appearance was better predicted by increasing the optimum temperature (Topt) by 3–4°C. The temperature dependency of rate of progress to anthesis and maturity was unchanged from canola because Jing et al. (2016) found the temperature functions worked well for canola. For leaf photosynthesis, the optimum temperature for the leaf rate was increased from 25 to 30°C with less reduction at higher temperature. This was needed to successfully simulate growth during the relatively warm month of May at these sites. Not listed in Table 3 is the effect of minimum night temperature (T_{min}) on the next day's photosynthesis. A two-point asymptotic function (−4°C and +7°C) describes the point of zero rate (when T_{min}

TABLE 3 Cardinal temperatures (°C): base (T_b), first optimum (T_{opt1}), second optimum (T_{opt2}), and ceiling failure (T_{ceil}) used for development, photosynthesis, pod addition, and seed growth rate of CROPGRO-Carinata compared to default for CROPGRO-Canola. Development functions use hourly temperatures with linear lookup with interpolation, while pod addition and seed growth rate use quadratic function on hourly temperature

	Carinata				Canola			
Growth/development process	T_b	T_{opt1}	T_{opt2}	T_{ceil}	T_b	T_{opt1}	T_{opt2}	T_{ceil}
Vegetative development	5	25	29	39	5	22	25	35
Reproductive development	0	21	25	35	0	21	25	35
Light saturated leaf photosynthesis	0	30	31	39	0	25	28	35
Leaf area expansion	0[a]	10[b]	20	—[c]	0[d]	10[b]	20	—[c]
Height/width increase	0[e]	10[f]	20	—[c]	0[e]	10[f]	20	—[c]
Pod and seed addition	2	12	20.3	29.8	0	9.5	20.3	29.8
Seed growth rate	1	15	24.5	35.5	0	14	24.5	35.5

[a]Relative expansion of 0.23 at 0°C.

[b]Relative expansion of 0.80 at 10°C.

[c]No ceiling temperature used.

[d]Relative expansion of 0.25 at 0°C.

[e]Relative internode increase of 0.40 at 0°C.

[f]Relative internode increase of 0.50 at 10°C.

is −4°C or less) to unlimited maximum rate (if T_{min} is +7°C or above). That function had been −3°C and +8°C for canola. For rate of pod and seed addition, the base temperature (T_b) and T_{opt1} were increased by 2°C, while the T_b and T_{opt1} for seed growth were increased by 1°C, both to improve model performance. Leaf area expansion and internode elongation are temperature-dependent processes that were not changed. Those expansion processes are reduced when hourly temperatures are less than 20°C, using the linear look-up function in Table 3.

3.2 | Model adaptation—Tissue compositions, protein, oil, and tissue N dynamics

Because CROPGRO can simulate N uptake from the soil as a non-legume, the N balance in the model requires setting critical tissue N (protein) compositions of the different organs. The model requires setting the approximate compositions of the different organs in terms of proteinaceous, cellulose-carbohydrate, lipid, lignin, organic acid, and ash, because it computes growth respiration following the approach of Penning deVries et al. (1974). The lipid, lignin, organic acid, and ash compositions remained as set for canola, but protein composition was modified, as shown in Table 4, based on comparison to observed vegetative N concentration of the Jay site experiments (N concentration data were not available for the Quincy and Shorter experiments). The canola default value for luxury protein of leaf (PROLFI) was much too high at 0.418 (mass/unit tissue mass), and was reduced to 0.340, while the luxury protein of stem (PROSTI) was reduced slightly from 0.274 to 0.264. Concurrently the luxury protein of pod (wall) was increased from 0.071 to 0.121 to be more accurate for this modified leaf structure. The "luxury" protein values represent the upper limit of protein in tissues under high "luxury" N supply. These two changes are likely also needed for the canola model. The cellulose-carbohydrate fraction was adjusted up or down, because it is the complement that changes when protein is parameterized (and indeed, also during the simulations when N deficit causes tissue protein to be reduced in any vegetative organ). Seed protein and lipid concentrations were separately parameterized at 0.300 and 0.440, respectively (see cultivar file, Table 5), and can vary under N deficit and in response to temperature. We have low confidence in these two effects on seed composition, as the code was created initially for soybean (*Glycine max* (L.) Merr.).

The CROPGRO model makes use of the PROLFI, PROLFG, and PROLFF (defined in Table 4) in the following manner during N balance dynamics. The PRO__I values for tissues set the growth demand for N uptake, and if daily root N uptake is not limiting, then new tissues are grown at this high "luxury" value each day. As daily N uptake reaches sufficient uptake to meet daily N demand, then new tissues are grown at the PROLFG concentration. When daily N uptake is not sufficient to grow at PROLFG concentrations, tissue N concentration is reduced, growth is reduced, and carbohydrate accumulates in leaves and stems (allocated by a ratio of 0.78 to stem and 0.22 to leaf). This accumulated carbohydrate pool is mobilized at relative rate of 0.035 per day, and can be used later when N uptake recovers. Simulated daily N uptake may not match daily photosynthesis, thus resulting in a fluctuating N stress (ratio of N supply to N demand). N stress also

TABLE 4 CROPGRO tissue compositions (mass per unit tissue dry mass), definitions, initial (canola) values, and calibrated carinata values for leaf, stem, shell, and seed

		Tissue–Initial values from canola				
Compound		**Leaf (LF)**	**Stem (ST)**	**Root (RT)**	**Shell (SH)**	**Seed (SD)**
PRO_ _I	Protein (luxury)	0.418	0.274	0.079	0.071	0.230
PRO_ _G	Protein (grow)	0.210	0.170	0.065	0.066	
PRO_ _F	Protein (final)	0.160	0.054	0.048	0.053	
PCAR_ _	Carbohydrate-cellulose	0.620	0.640	0.710	0.660	0.220
PLIP_ _	Lipid	0.040	0.011	0.008	0.019	0.480
PLIG_ _	Lignin	0.011	0.011	0.011	0.011	0.060
POA_ _	Organic acid	0.036	0.024	0.036	0.036	0.010
PMIN_ _	Mineral	0.081	0.035	0.045	0.042	0.010
		Tissue–Calibrated values for carinata				
Compound		**Leaf (LF)**	**Stem (ST)**	**Root (RT)**	**Shell (SH)**	**Seed (SD)**
PRO_ _I	Protein (luxury)	0.340	0.264	0.075	0.121	0.300
PRO_ _G	Protein (grow)	0.210	0.170	0.060	0.076	
PRO_ _F	Protein (final)	0.160	0.054	0.048	0.053	
PCAR_ _	Carbohydrate-cellulose	0.492	0.655	0.825	0.771	0.180
PLIP_ _	Lipid	0.040	0.011	0.008	0.019	0.440
PLIG_ _	Lignin	0.011	0.011	0.011	0.011	0.060
POA_ _	Organic acid	0.036	0.024	0.036	0.036	0.010
PMIN_ _	Mineral	0.081	0.035	0.045	0.042	0.010

TABLE 5 Genetic coefficients of carinata, Avanza-641 cultivar, as defined in the cultivar file of the CROPGRO model, after calibration, and compared to canola

Genetic coefficients	**Carinata**	**Canola**[a]
Critical long daylength above which reproductive development progresses as rapidly as possible with no daylength effect (CLDL) (h)	16.00	16.00
Slope of the relative response of development versus photoperiod (PP-SEN) (1 h^{-1})	−0.012	−0.011
Time between emergence and flower appearance (EM-FL) (ptd)	42.0	28.5
Time between first flower and beginning rachis/bud/pod (FL-SH) (ptd)	8.0	13.0
Time between first flower and beginning seed (FL-SD) (ptd)	19.5	19.0
Time between beginning seed and (beginning) physiological maturity (SD-PM) (ptd)	38.5	26.5
Time between first flower and last leaf expansion (FL-LF) (ptd)	7.00	3.00
Maximum leaf photosynthetic rate at 30°C, 350 μL L^{-1} CO_2, and high light (LFMAX) (mg CO_2 m^2 s^{-1})	1.11	1.28
Specific leaf area of cultivar under standard growth conditions (SLAVAR) (cm^2 g^{-1})	280.0	300.0
Maximum size of fifth full leaf (SIZLF) (cm^2)	95.0	100.0
Maximum fraction of daily growth that is partitioned to seed + shell (XFRT)	0.96	1.00
Maximum weight per seed (WTPSD) (g)	0.006	0.003
Seed-filling duration for seed cohort under standard conditions (SFDUR) (ptd)	27.0	36.0
Seed number per pod (SDPDV)	9.0	22.0
Duration of pod addition under standard conditions (PODUR) (ptd)	11.3	10.0
Threshing percentage [seed (seed + shell)$^{-1}$] (THRSH)	63.0	81.0
Fraction protein in seeds (SDPRO) [g (protein) g (seed)$^{-1}$]	0.300	0.230
Fraction oil in seeds (SDLIP) [g (oil) g (seed)$^{-1}$]	0.440	0.480

Abbreviation: ptd, Photothermal days.

[a]Genetic coefficients for canola from Jing et al. (2016).

triggers an increase of assimilate allocation to roots (Boote et al., 2009). The model has a relative rate of N mobilization (NMOBMX) from all vegetative tissues, which drives N mobilization from old to new leaves, and this is increased during seed growth. The NMOBMX is 0.205 (during seed-fill), but is less by the fraction (NVSMOB = 0.20) during the vegetative phase prior to seed growth (thus giving a relative rate of 0.041 per thermal day during vegetative). The N dynamics of the CROPGRO model are described in detail by Boote et al. (2009).

3.3 | Model adaptation—Setting cultivar traits

Cultivar traits defined in Table 5 for carinata (cv. Avanza-641) are compared to canola cv. Kabel. Compared to canola, we assumed similar sensitivity to daylength (long days accelerate progress), but carinata required more photothermal days (ptd) to first flower (EM-FL). Photothermal days are a function of thermal days using the relative temperature sensitivity in Table 3 multiplied by the daylength sensitivity in Table 5. One ptd is accumulated in one calendar day if daylength is longer than the critical long daylength (CLDL in Table 5) and the temperature is optimum all day (between T_{opt1} and T_{opt2}). The ptd accumulated during a calendar day will be less than 1.0 if daylength is less than CLDL and temperature is not optimum. Using EM-FL of 42 ptd resulted in the correct flowering date, and along with FL-SH (8.0 ptd from first flower to first pod) and FL-SD (19.5 ptd from first flower to onset of seed), gave correct observed onset of pod and seed mass growth for the Quincy location (other sites lacked sufficient pod and seed sampling). The time to maturity was poorly observed in the field because the phenology observations were infrequent (biweekly) and lacked the precision needed to determine when the first seeds matured and when most of the seeds (e.g., 90%) were mature. So the SD-PM parameter (38.5 ptd) for the onset of seed growth until physiological maturity was set approximately based on achieving maximum pod and seed mass based on biweekly growth samples. The light-saturated leaf photosynthesis rate (LFMAX) value in Table 5 was set typical of C-3 species, and is close to unpublished values measured at Jay (personal communications, M. Bashyal and Noia Junior). The SLAVR (Table 5) was calibrated from the SLA values over time and was comparable

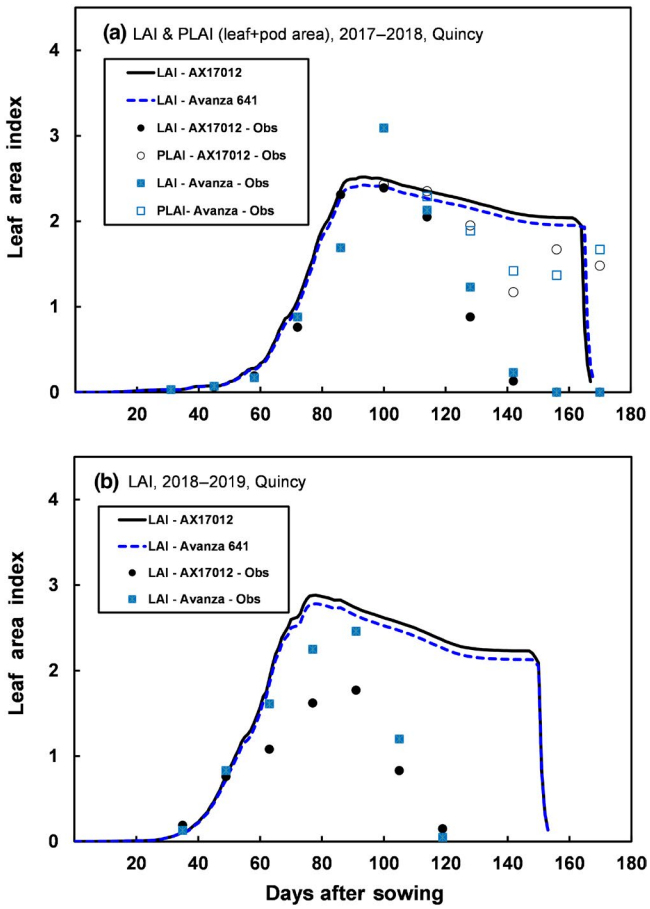

FIGURE 1 Simulated (lines) and observed (points) leaf area index and pod area index over time for two cultivars in: (a) 2017–2018 season, and (b) 2018–2019 season at Quincy, FL

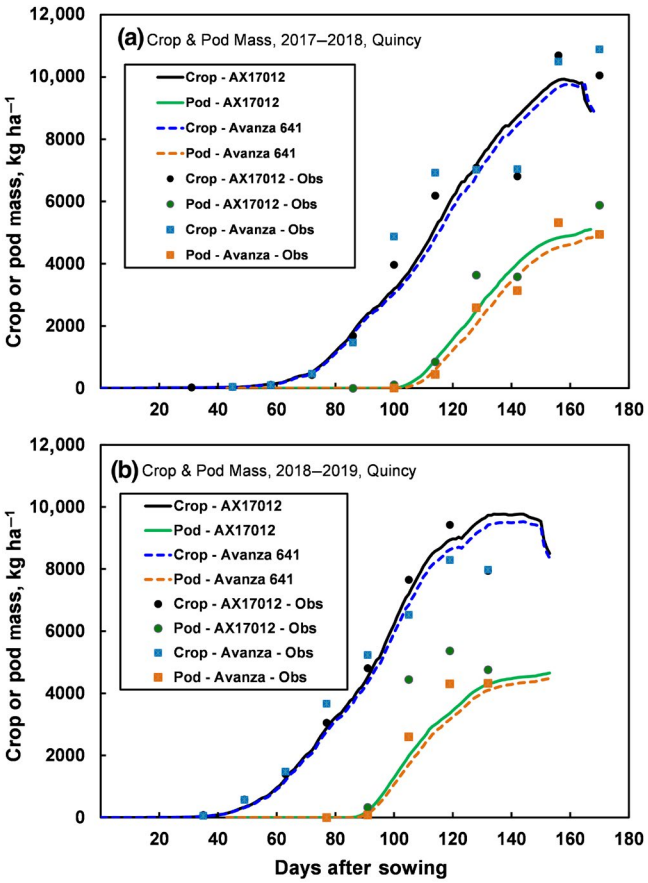

FIGURE 2 Simulated (lines) and observed (points) crop and pod mass over time for two cultivars in: (a) 2017–2018 season and (b) 2018–2019 season at Quincy, FL

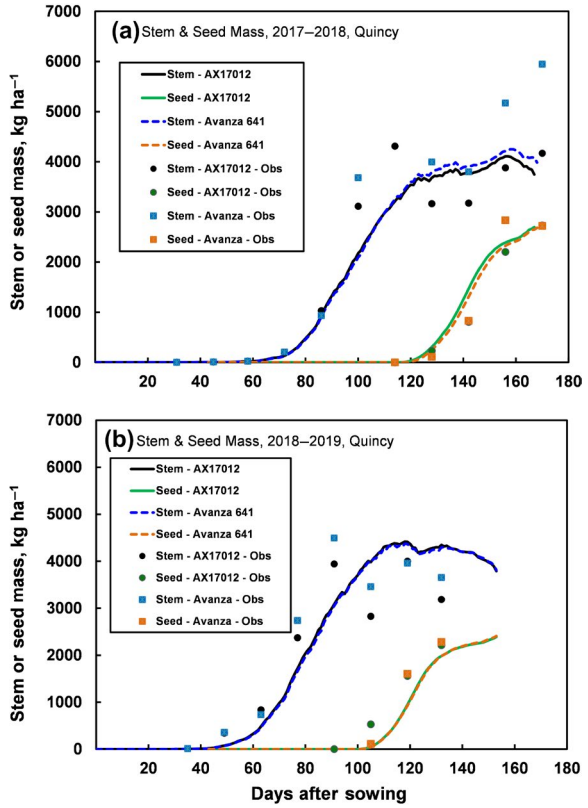

FIGURE 3 Simulated (lines) and observed (points) stem and seed mass over time for two cultivars in: (a) 2017–2018 season and (b) 2018–2019 season at Quincy, FL

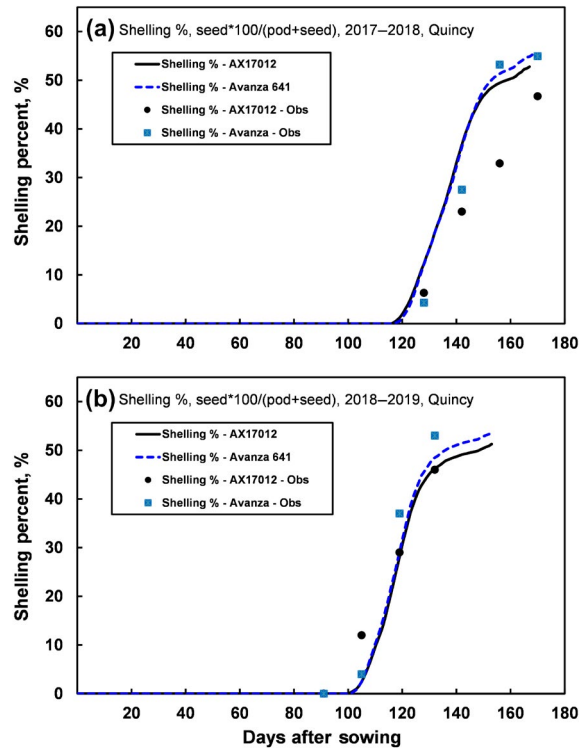

FIGURE 4 Simulated (lines) and observed (points) shelling percentage (seed × 100%/(seed + podwall)) over time for two cultivars in: (a) 2017–2018 season and (b) 2018–2019 season at Quincy, FL

to that for canola. The XFRT value of 0.96 (Table 5) was set based on the time course and final magnitude of pod harvest index, along with fitting the stem, pod, and seed mass accurately. An XFRT of 1.00 implies total physiological determinacy. The PODUR of 11.3 ptd was needed to create a sufficiently rapid rise in the pod harvest index over time, and compares to 10 ptd for canola. THRESH was calibrated at 63% for Avanza-641 from the final shelling percentage of pods as well as the time course of shelling percentage. The SFDUR parameter was set to 27 ptd to mimic the rapid rise in the shelling percentage over time. We believe the THRESH value and the long SFDUR for canola are incorrect, but may compensate for each other. SDLIP and SDPRO were set to mimic final seed composition based on Jay, FL data.

3.4 | Model evaluation: Time course dynamics of LAI, biomass, pod, stem, and seed

The Quincy location had the most complete data, particularly for LAI and partitioning to leaf, stem, pod, and seed. Figure 1 illustrates the LAI for the Avanza-641 and AX17012

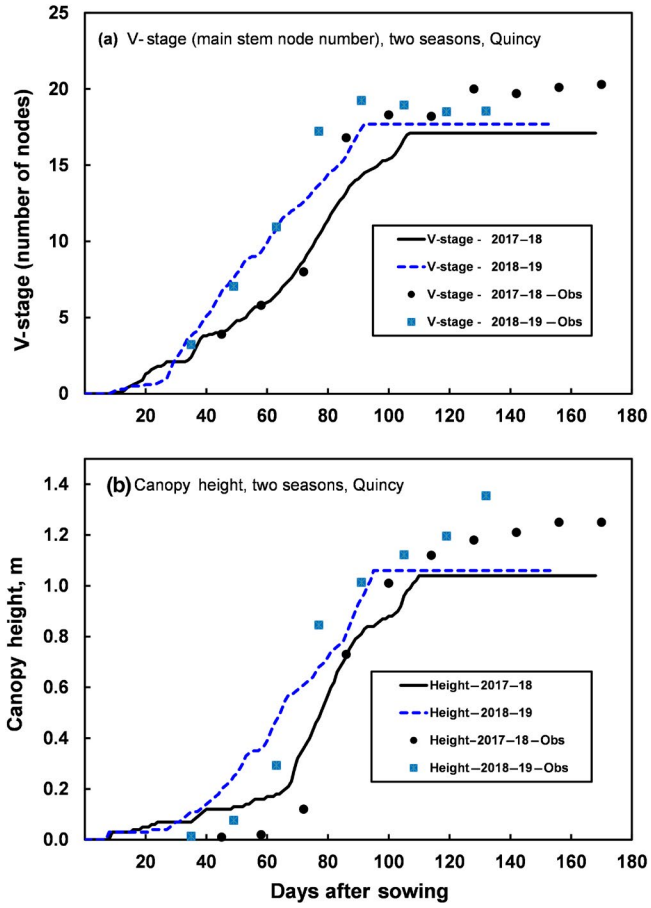

FIGURE 5 Simulated (lines) and observed (points) for: (a) Mainstem node number (V-stage) and (b) canopy height over time for Avanza-641 cultivar in 2017–2018 and 2018–2019 seasons at Quincy, FL

cultivars in two seasons. Model simulated LAI was calibrated to match observed LAI only during the first half of the life cycle, similar to the approach of Jing et al. (2016) for canola, because leaves begin to senesce and abscise relatively early during seed-filling as reported by Gammelvind et al. (1996), yet there is considerable green pod area at the top of the canopy that intercepts radiation and performs photosynthesis. Jing et al. (2016) used a photographic technique to estimate total plant area index, comprised of green leaves, pods, and stems. They concluded that green pods contributed to canopy photosynthesis. Therefore, they calibrated LAI to mimic observed total plant area index, thus creating a mimic of a "false" simulated LAI that remained relatively high from its peak until maturity despite the loss of leaves. We measured only observed LAI at Quincy and Jay in the two seasons, but we were able to separately measure the pod area index in the 2017–2018 season at Quincy, FL; thus, Figure 1a shows reasonable model simulations against the sum of leaf area plus pod area. Therefore, we followed the approach of Jing et al. (2016) to obtain accurate predictions only for the earliest two-thirds of the season (evident in Figure 1a,b), and to allow a "false" over-prediction of LAI and leaf mass for the latter part of the season only. We measured photosynthesis of leaves averaging 0.97, 1.08, and 1.17 mg CO_2 m^{-2} s^{-1} for 0, 90, and 180 kg N ha^{-1} treatments during the 2018–2019 season at Jay. These rates closely match the LFMAX input of 1.11 mg CO_2 m^{-2} s^{-1} for Avanza 641. Measured rates on green pods averaged 0.40 mg CO_2 m^{-2} s^{-1}, a rate that is 37% of leaves. Gammelvind et al. (1996) measured photosynthesis of leaves and green pods of winter oilseed rape, and found that pods had a rate 38% that of leaves. We did not include photosynthesis of green pods in our simulations explicitly, but we conclude that photosynthesis of green pods is important to consider for future code modification similar to that done by Timsina et al. (2007).

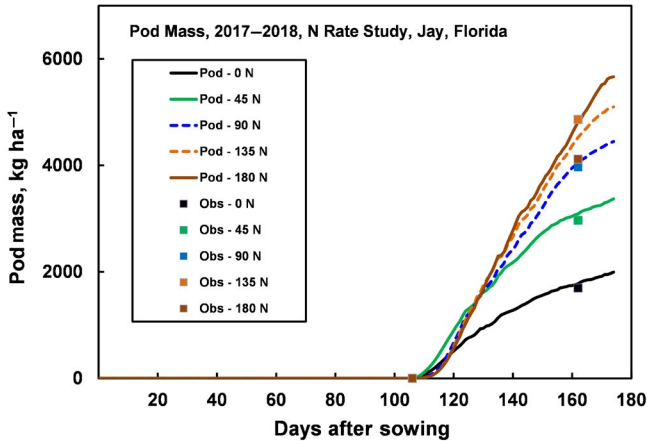

FIGURE 6 Simulated (lines) and observed (points) pod mass over time for N rate treatments in 2017–2018 at Jay, FL

The crop biomass and pod mass were well simulated for Quincy for 2017–2018 (Figure 2A) and 2018–2019 (Figure 2B). The 2017–2018 season was longer and more delayed because of earlier sowing and cooler winter temperatures. The two cultivars, Avanza 641 and AX17012, had relatively similar performance for biomass, although AX17012, having been selected for early maturity, was earlier for pod growth (FL-SH = 6.6 ptd, FL-SD = 19.0 ptd) and was somewhat more determinate (XFRUIT of 0.97 vs. 0.96) with shorter time for pod addition of 11.2 ptd versus 11.3 ptd. AX17012 was assigned a higher leaf photosynthesis (LFMAX of 1.15 compared to Avanza 641 at 1.11), but the difference was small. Figure 3a,b show that the AX17012 cultivar was somewhat more determinate with slightly earlier onset of seed and less stem mass than Avanza, but the difference in seed growth was small. Figure 4a,b illustrate the shelling percentage of the two cultivars in the two seasons at Quincy. Shelling percentage is seed mass divided by the mass of podwall + seed, defined as percentage. The genetic potential shelling percentage (THRESH) of AX17012 was less than that of Avanza (62 vs. 63%), but the difference is small and would have minor effects on yield. This was calibrated to time series as well as final shelling percentage at maturity.

TABLE 6 V-stage dependencies: vegetative partitioning to leaf, stem, and root; and canopy internode height and width parameters as a function of main stem leaf number (XLEAF is same as V-stage)

XLEAF	0.0	5.0	7.5	10.0	12.0	14.0	16.0	18.0	Final	
YLEAF[a]	0.74	0.69	0.51	0.42	0.27	0.15	0.08	0.08	0.06	
YSTEM[a]	0.05	0.10	0.24	0.40	0.59	0.71	0.78	0.78	0.82	
YROOT[a]	0.21	0.21	0.25	0.18	0.14	0.14	0.14	0.14	0.12	
XLEAF	**0.00**	**1.00**	**4.00**	**6.00**	**8.00**	**10.00**	**14.00**	**16.00**	**20.00**	**40.00**
YVSHT[b]	0.0250	0.0270	0.0290	0.0340	0.0660	0.0850	0.0850.	0.0780	0.0630	0.0080
YVSWH[c]	0.0290	0.0360	0.0440	0.0540	0.0600	0.0600	0.0550	0.0450	0.0200	0.0010

[a]Fraction partitioning.

[b]Internode length, m.

[c]Width, m.

3.5 | Model evaluation: Height, width, and partitioning among vegetative components are a function of V-stage progression

The number of fully expressed leaf nodes on the main stem over time was measured at all three sites, and is shown in Figure 5a for two seasons for Avanza 641 at Quincy. The cool weather effect of delayed node appearance was obvious during 2017–2018, but the final main stem node number was the same at 18–19. AX17012 had a very similar rate of node appearance and final node number as Avanza 641. The rate of leaf appearance is well simulated based on the TRIFL parameter of 0.42 (rate of leaf appearance per thermal day) and the cardinal temperatures given in Table 3. Simulating the vegetative stage (number of leaves on the main axis, XLEAF = V-Stage) is a useful type of thermal accumulator in the model. Vegetative stage is important to several functions in the model: (1) it allows phenological control of fraction daily partitioning to leaf, stem, and root growth, (2) it drives canopy height and width, which can be calibrated by setting internode length against main stem node number (the arrays in Table 6). The rates of height and width increase over time are important for creating hedgerow canopy size for light capture. Figure 5b illustrates the canopy height increase for Avanza 641 for the two seasons in Quincy. Height increase is slow early because of rosette growth behavior along with cool temperatures, but then height increases rapidly after 60–70 days after six to eight nodes have appeared, but reaches a determinate plateau when final node number is expressed. The model is sensitive to plant population and row spacing (but that is not testable with present data). The model ability to simulate canopy height and width would mimic lower light capture and production as the row spacing becomes greater.

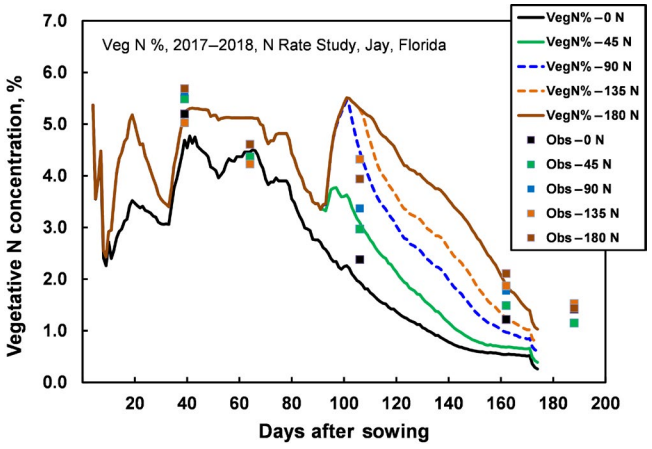

FIGURE 7 Simulated (lines) and observed (points) vegetative N concentration over time for N rate treatments in 2017–2018 at Jay, FL

TABLE 7 Comparison of means of observed and simulated crop variables over all time-series data over 2 years at three sites, n = number of observations, root mean square error (RMSE), and d-statistic

Crop variable	Number of observations[a]	Observed mean	Simulated mean	RMSE	d-statistic
Leaf area index (LAI)	4	1.283	1.309	0.705	0.672
Specific leaf area (SLA), $cm^2\ g^{-1}$	4	245.7	248.2	57.0	0.358
Total crop mass, kg DM ha^{-1}	5	3321	3107	1062	0.966
Stem mass, kg DM ha^{-1}	5	2685	2133	1107	0.777
Leaf mass, kg DM ha^{-1}	5	548	693	398	0.533
Pod mass, kg DM ha^{-1}	5	2210	2440	706	0.906
Seed yield, kg DM ha^{-1}	2	1294	1138	421	0.949
Pod harvest index	5	0.272	0.316	0.122	0.864
Seed harvest index	2	0.149	0.126	0.048	0.937
Shelling percentage, %	2	29.83	29.97	6.09	0.974
Node number (V-stage)	6	8.20	8.45	1.75	0.905
Canopy height (m)	5	0.835	0.828	0.142	0.641
N Rate study at Jay, Florida					
Veg N over time, % of DM	10	3.22	3.39	0.707	0.872
Crop N over time, kg N ha^{-1}	10	46.3	54.2	32.5	0.880
Crop mass over time, kg ha^{-1}	10	2332	2214	1337	0.936
Final seed yield, kg ha^{-1}	10	2138	2198	473	0.919
Seed oil, % of DM	5	43.3	44.2	1.00	0.440
Seed N, % of DM	5	4.21	3.92	0.42	0.235

[a]For sites with five observations, the Shorter, AL 2018–2019 season was deleted.

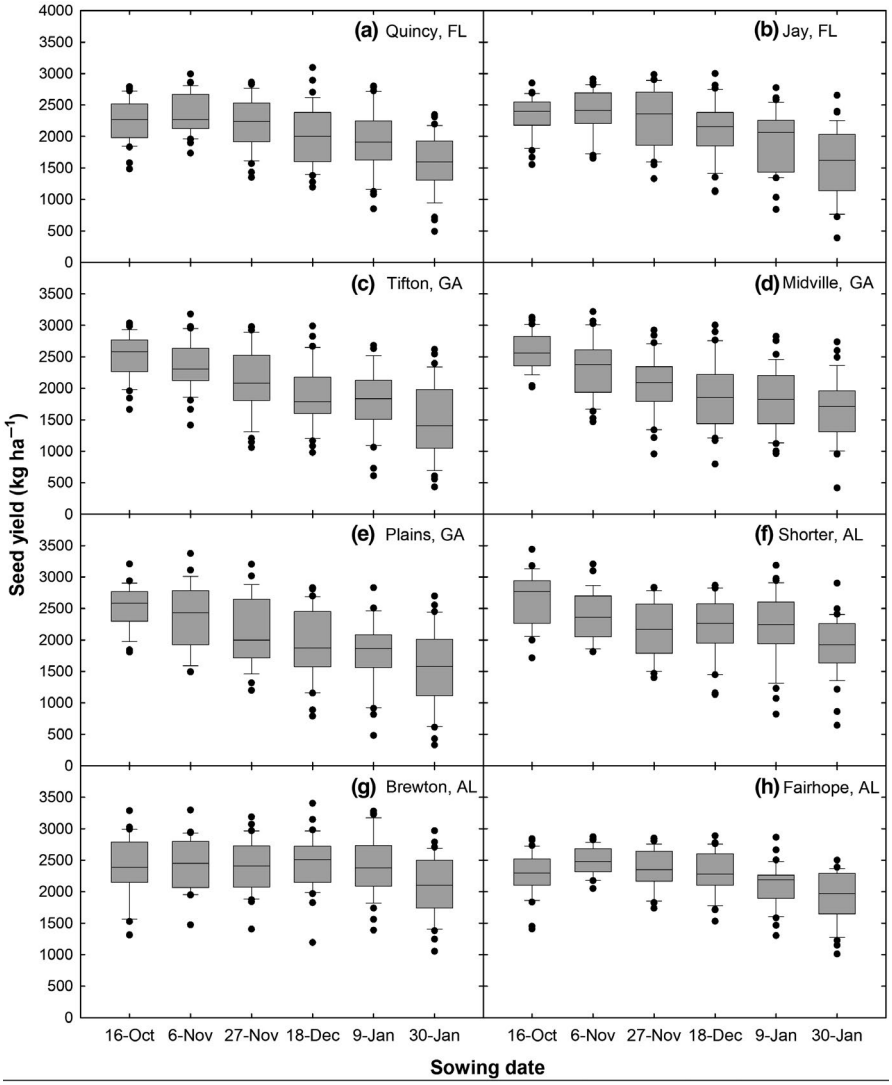

FIGURE 8 Effect of sowing date on simulated seed yield of carinata over 35 years at eight sites in Florida, Georgia, and Alabama. Plots show median (horizontal line), 25–75 percentile (box), 10–90 percentile (vertical line), and outlier points

Important to the model is that partitioning among leaf, stem, and root are controlled as a function of V-stage (number of mainstem leaves). Partitioning to leaf is high and that to stem is low for seedling plants, whereas after the plant reaches V7, the partitioning to stem increases rapidly and that to leaf rapidly declines. Root receives the complement (100 minus partitioning to leaf and stem), and is programmed to decline over time, being about 12% of the daily assimilate by the beginning seed-fill. The partitioning look-up function in Table 6 describes the allocation among vegetative tissues; but in fact, once pods and seeds begin to grow, those reproductive organs have first priority for assimilates; thus, the leaf, stem, and root share in any remainder (possibly reaching zero by the time of a full seed load).

3.6 | Model evaluation: Response to N fertilization at Jay site

The growth and yield responses to N fertilization were evaluated at the Jay site. The model, with parameterization of the stable C pool of CENTURY at 78% of total organic C, was successful in simulating the pod yield response to the five N fertilization rates (Figure 6). The model also satisfactorily reproduced the vegetative N concentration over time for the different treatments (Figure 7).

3.7 | Model evaluation: Statistical evaluation of model simulations

Table 7 lists the simulated and observed means, RMSE, and d-statistics for time-series observations across 2 years over three sites after model adaptation. The number of observations in the time-series simulations varies because only biomass was measured at all sites, while pod and LAI were measured over 2 years at two sites (not Shorter, AL). All sites and years of data were used for model calibration. Most of the time-series crop variables were well simulated with a d-statistic exceeding 0.90, especially the total crop biomass with d-statistic of 0.936 for Jay location and 0.966 for 5-treatment set (Quincy, Jay, Shorter). Pod mass over time was well simulated with a d-statistic of 0.906. Exceptions include LAI, leaf, stem, and SLA, but there

are reasons for the statistical disagreement on these vegetative components because we intentionally overestimated leaf weight and LAI during seed-filling to offset early leaf abscission, while stem is likely too low to offset the fact that simulated leaf and LAI were maintained high (thus giving total biomass a good fit). The simulation of vegetative N concentration and total N accumulation for the 10 treatments of the N rate study at Jay showed acceptable outcomes with d-statistics of 0.872 and 0.880, respectively. This shows promise that the model can capture N response adequately, although setting CENTURY's soil organic C pools will always be a soil-specific issue. Simulated seed oil concentration was 44.2% compared to 43.3% observed.

3.8 | Regional application: Simulated response to sowing dates at eight Southeastern US sites

Simulated seed yield and maturity date are shown in Figures 8 and 9 for six sowing dates at eight sites in the Southeastern USA. The interannual distribution of yield and maturity are caused by seasonal variation in temperature and rainfall. Simulated yields were generally higher for the earlier sowing dates. The October 16 date gave the highest yield for five of the eight sites, although the November 6 date was highest yielding at three sites (Figure 8). With yields in the median range of 2200–2800 kg ha^{-1} and oil at 46%, the simulated oil yields would range from 1100 to 1400 L ha^{-1}. For the more northerly locations (Tifton, Midville, Plains, Shorter, Brewton), it is reasonable to recommend sowing between October 16 and November 6, both to achieve high yield, and to avoid maturity later than May 31 (day of year 151 in Figure 9). Timely maturity and harvest are important to allow second crops, such as cotton, peanut, soybean, and sorghum to follow. For the more southerly sites closer to the Gulf (Quincy, Jay, and Fairhope), the sowing date range for high yield and reasonable maturity is broader and stretches from October 16 to November 27. Table S1 gives the mean, minimum, maximum yields, and times to maturity for these sowing dates

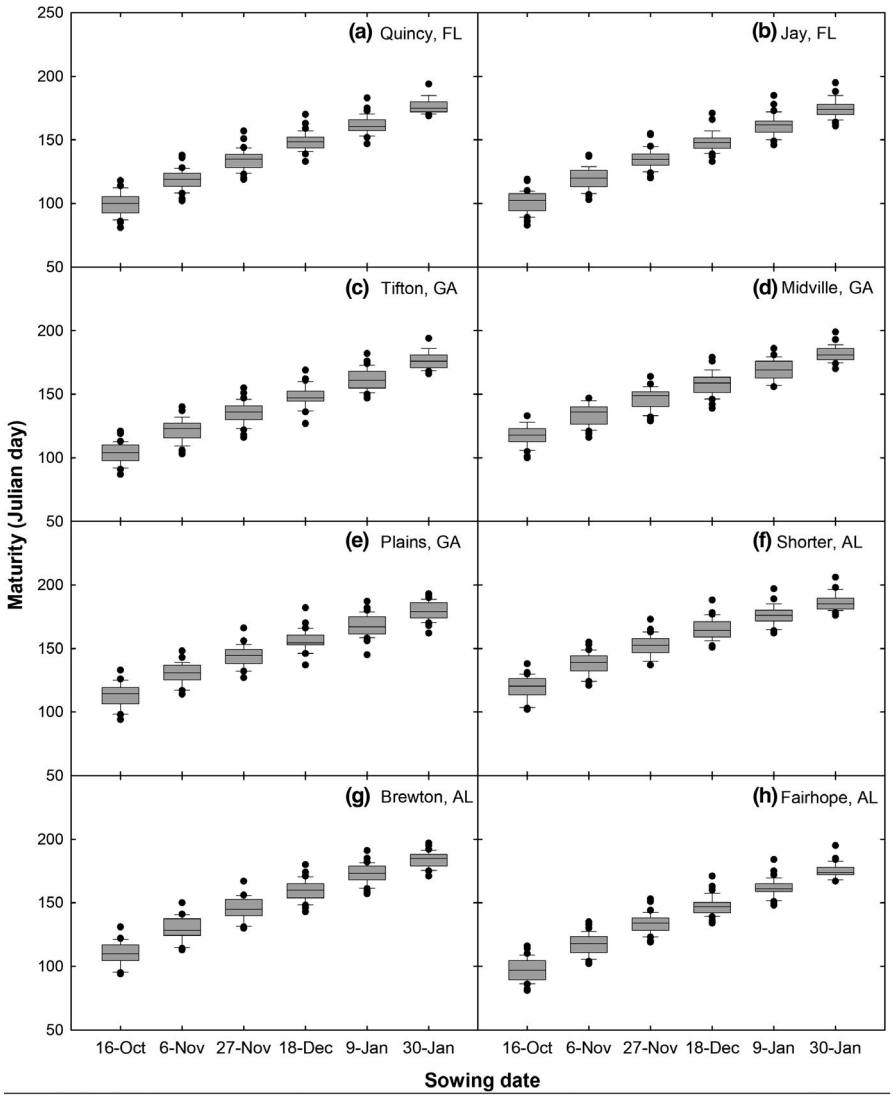

FIGURE 9 Effect of sowing date on simulated maturity dates (day of year) of carinata over 35 years at eight sites in Florida, Georgia, and Alabama. Plots show median (horizontal line), 25–75 percentile (box), 10–90 percentile (vertical line), and outlier points

at eight sites as well as the risk of freeze kill assuming a threshold of −11°C. The simulated freeze risk is greater for Plains, Shorter, and Brewton, but caution is warranted here, as the parameterization of the killing temperature is somewhat uncertain. In addition, the life cycle progression and maturity dates depend on temperature and daylength, but definitive research on the cardinal temperatures is lacking, and the extent of long-day acceleration of life cycle, while parameterized, is also uncertain. Additional research on these factors is needed along with additional field data, to facilitate future model improvement.

4 | CONCLUSIONS

The CROPGRO-Carinata model was successfully adapted based on growth analyses data from three sites. The adapted model provided good simulations of growth dynamics of carinata during different seasons and locations and in response to N fertilization. Model application illustrates reasonable yield and maturity responses to sowing date, allowing to recommend that sowing should be timely (in late October to early November) for high yield and sufficiently early maturity to fit with following summer row crops. While additional testing is appropriate, the model is sufficiently ready to be placed in the DSSAT system and to be used for various applications to evaluate management strategies and weather effects on the production of carinata. The model and these data are appropriate to use for carinata production in the Southeastern USA as this promising commodity comes to market.

ACKNOWLEDGEMENTS

This work was supported in part by the National Institute of Food and Agriculture, U.S. Department of Agriculture-USDA National Institute of Food and Agriculture, under award number 2016-11231 and by the USDA National Institute of Food and Agriculture, Hatch projects 1022754 and 1022353. We acknowledge and thank Daniel Perondi, University of Florida graduate student, for providing the long-term weather for these sites and soil information for five sites.

DATA AVAILABILITY STATEMENT

The data used in this paper and the developed Carinata model will be available to the public after publication, available as files and model code/parameters placed in the free and downloadable DSSAT software system.

ORCID

Kenneth J. Boote https://orcid.org/0000-0002-1358-5496
Ramdeo Seepaul https://orcid.org/0000-0001-6246-0385
Mahesh Bashyal https://orcid.org/0000-0001-5882-5353
Sheeja George https://orcid.org/0000-0001-9046-683X

REFERENCES

Alderman, P. D., Boote, K. J., Jones, J. W., & Bhatia, V. S. (2015). Adapting the CSM-CROPGRO model for pigeonpea using sequential parameter estimation. *Field Crops Research*, *181*, 1–15.

Allen, R. G., Pereira, L. S., Raes, D., & Smith, M. (1998). *Crop evapotranspiration. Guidelines for computing crop water requirements*. FAO Irrig. and Drainage Paper no. 56. FAO.

Boote, K. J., Hoogenboom, G., Jones, J. W., & Ingram, K. T. (2009). Modeling N-fixation and its relationship to N uptake in the CROPGRO model. In L. Ma, L. Ahuja, & T. Bruulsema (Eds.), *Quantifying and understanding plant nitrogen uptake for systems modeling* (pp. 13–46). Taylor & Francis Group LLC.

Boote, K. J., Jones, J. W., & Hoogenboom, G. (1998). Simulation of crop growth: CROPGRO model. Chapter 18. In R. M. Peart & R. B. Curry (Eds.), *Agricultural systems modeling and simulation* (pp. 651–692). Marcel Dekker, Inc.

Boote, K. J., Mínguez, M. I., & Sau, F. (2002). Adapting the CROPGRO legume model to simulate growth of faba bean. *Agronomy Journal*, *94*, 743–756.

Boote, K. J., & Pickering, N. B. (1994). Modeling photosynthesis of row crop canopies. *HortScience*, *29*, 1423–1434.

Boote, K. J., Rybak, M. R., Scholberg, J. M. S., & Jones, J. W. (2012). Improving the CROPGRO-Tomato model for predicting growth and yield response to temperature. *HortScience*, *47*, 1038–1049.

Boote, K. J., Sau, F., Hoogenboom, G., & Jones, J. W. (2008). Experience with water balance, evapotranspiration, and prediction of water stress effects in the CROPGRO model. In L. R. Ahuja, V. R. Reddy, S. A. Saseendran, & Q. Yu (Eds.), *Response of crops to limited water: Modeling water stress effects on plant growth processes, volume 1 of advances in agricultural systems modeling* (pp. 59–103). ASA-CSSA-SSSA.

Cardone, M., Mazzoncini, M., Menini, S., Rocco, V., Senatore, A., Seggiani, M., & Vitolo, S. (2003). *Brassica carinata* as an alternative oil crop for the production of biodiesel in Italy: Agronomic evaluation, fuel production by transesterification and characterization. *Biomass and Bioenergy*, *25*, 623–636.

Deligios, P. A., Farci, R., Sulas, L., Hoogenboom, G., & Ledda, L. (2013). Predicting growth and yield of winter rapeseed in a Mediterranean environment: Model adaptation at a field scale. *Field Crops Research*, *144*, 100–112.

Farquhar, G. D., & von Caemmerer, S. (1982). Modeling of photosynthetic response to environment. In O. L. Lange et al (Eds.), *Encyclopedia of plant physiology. New series. Vol. 12B. Physiological plant ecology II* (pp. 549–587). Springer-Verlag.

Gammelvind, L. H., Schjoerring, J. K., Mogensen, V. O., Jensen, C. R., & Bock, J. G. H. (1996). Photosynthesis in leaves and siliques of winter oilseed rape (*Brassica napus* L.). *Plant and Soil*, *186*, 227–236.

Gijsman, A. J., Hoogenboom, G., Parton, W. J., & Kerridge, P. C. (2002). Modifying DSSAT crop models for low-input agricultural systems using a soil organic matter–residue module from CENTURY. *Agronomy Journal*, *94*, 462–474.

Hoogenboom, G., Jones, J. W., Wilkens, P. W., Porter, C. H., Boote, K. J., Hunt, L. A., Singh, U., Lizaso, J. I., White, J. W., Uryasev, O., Ogoshi, R., Koo, J., Shelia, V., & Tsuji, G. Y. (2015). *Decision support system for agrotechnology transfer (DSSAT) version 4.6*. http://dssat.net. DSSAT Foundation.

Hoogenboom, G., Porter, C. H., Boote, K. J., Shelia, V., Wilkens, P. W., Singh, U., White, J. W., Asseng, S., Lizaso, J. I., Moreno, L. P., Pavan,

W., Ogoshi, R., Hunt, L. A., Tsuji, G. Y., & Jones, J. W. (2019). The DSSAT crop modeling ecosystem. In K. J. Boote (Ed.), *Advances in crop modelling for a sustainable agriculture* (pp. 173–216). Burleigh Dodds Science Publishing.

Jing, Q. I., Shang, J., Qian, B., Hoogenboom, G., Huffman, T., Liu, J., Ma, B.-L., Geng, X., Jiao, X., Kovacs, J., & Walters, D. (2016). Evaluation of the CSM-CROPGRO-Canola Model for simulating canola growth and yield at West Nipissing in eastern Canada. *Agronomy Journal*, *108*, 575–584.

Jones, J. W., Antle, J. M., Basso, B., Boote, K. J., Conant, R. T., Foster, I., Godfray, H. C. J., Herrero, M., Howitt, R. E., Janssen, S., Keating, B. A., Munoz-Carpena, R., Porter, C. H., Rosenzweig, C., & Wheeler, T. R. (2017). Toward a new generation of agricultural system data, models, and knowledge products: State of agricultural systems science. *Agric Systems*, *155*, 269–288. https://doi.org/10.1016/j.agsy.2016.09.021

Jones, J. W., Hoogenboom, G., Porter, C. H., Boote, K. J., Batchelor, W. D., Hunt, L. A., Wilkens, P. W., Singh, U., Gijsman, A. J., & Ritchie, J. T. (2003). The DSSAT cropping system model. *European Journal of Agronomy*, *18*, 235–265.

Malik, R. S. (1990). Prospects for *Brassica carinata* as an oilseed crop in India. *Experimental Agriculture*, *26*(1), 125–130.

Penning de Vries, F. W. T., Brunsting, A. H. M., & van Laar, H. H. (1974). Products, requirements and efficiency of biosynthesis: A quantitative approach. *Journal of Theoretical Biology*, *45*, 339–377.

Priestley, C. H. B., & Taylor, R. J. (1972). On the assessment of surface heat and evaporation using large scale parameters. *Monthly Weather Review*, *100*, 81–92.

Ritchie, J. T. (1998). Soil water balance and crop water stress. In G. Y. Tsuji, G. Hoogenboom, & P. K. Thornton (Eds.), *Understanding options for agricultural production* (pp. 41–54). Kluwer Academic Press.

Seepaul, R., George, S., & Wright, D. L. (2016). Comparative response of *Brassica carinata* and *B. napus* vegetative growth, development and photosynthesis to nitrogen nutrition. *Ind. Crop. Prod.*, *94*, 872–883. https://doi.org/10.1016/j.indcrop.2016.09.054

Seepaul, R., Kumar, S., Iboyi, J. E., Bashyal, M., Stansly, T. L., Bennett, R., Boote, K. J., Mulvaney, M. J., Small, I. M., George, S., & Wright, D. L. (2021). *Brassica carinata*: Biology and agronomy as a biofuel crop. *GCB Bioenergy*, *2021*(13), 582–599. https://doi.org/10.1111/gcbb.12804

Seepaul, R., Marois, J., Small, I. M., George, S., & Wright, D. L. (2019). Carinata dry matter accumulation and nutrient uptake responses to nitrogen fertilization. *Agronomy Journal*, *111*, 2038–2046. https://doi.org/10.2134/agronj2018.10.0678

Seepaul, R., Small, I. M., Marois, J., George, S., & Wright, D. L. (2019). *Brassica carinata* and *Brassica napus* growth, nitrogen use, seed, and oil productivity constrained by post-bolting nitrogen deficiency. *Crop Science*, *59*, 2720–2732. https://doi.org/10.2135/cropsci2018.12.07422

Singh, S., Boote, K. J., Angadi, S. V., Grover, K., Begna, S., & Auld, D. (2015). Adapting the CROPGRO model to simulate growth and yield of spring safflower in semiarid conditions. *Agronomy Journal*, *108*, 64–72.

Timsina, J., Boote, K. J., & Duffield, S. (2007). Evaluating the CROPGRO Soybean model for predicting impacts of insect defoliation and depodding. *Agronomy Journal*, *99*, 148–157.

Willmott, C. J. (1982). Some comments on the evaluation of model performance. *Bulletin of the American Meteorological Society*, *63*, 1309–1313.10.1175/1520-0477(1982)063<1309:SCOTEO>2.0.CO;2

Willmott, C. J., Ackleson, S. G., Davis, R. E., Feddema, J. J., Klink, K. M., Legates, D. R., O'Donnell, J., & Rowe, C. M. (1985). Statistics for the evaluation and comparison of models. *Journal of Geophysical Research: Oceans*, *90*(C5), 8995–9005. https://doi.org/10.1029/JC090iC05p08995

SUPPORTING INFORMATION

Additional supporting information may be found online in the Supporting Information section.

How to cite this article: Boote KJ, Seepaul R, Mulvaney MJ, et al. Adapting the CROPGRO model to simulate growth and production of *Brassica carinata*, a bio-fuel crop. *GCB Bioenergy*. 2021;13:1134–1148. https://doi.org/10.1111/gcbb.12838